Journal of Hazardous Materials 380 (2019) 120625

Contents lists available at ScienceDirect

Journal of Hazardous Materials

journal homepage: www.elsevier.com/locate/jhazmat

Superhydrophobic and oleophobic ultra-fine dry chemical agent with higher chemical activity and longer fire-protection

Junchao Zhao, Zhitao Yin, Muhammad Usman Shahid, Haoran Xing, Xudong Cheng, Yangyang Fu*, Song Lu*

State Key Laboratory of Fire Science, University of Science of Technology of China, 230026, PR China

GRAPHICAL ABSTRACT

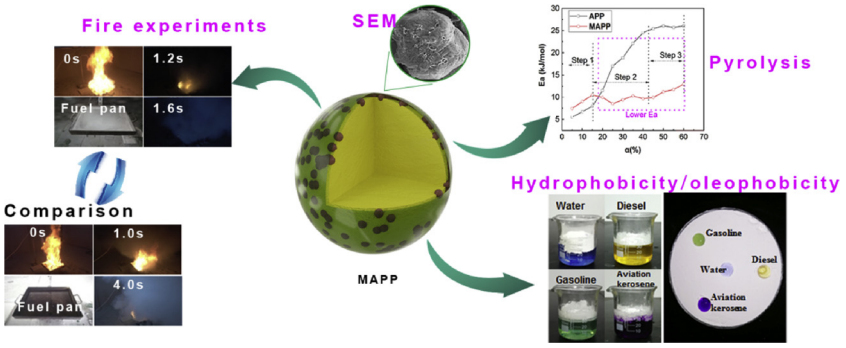

ARTICLE INFO

Keywords:
Superhydrophobic and oleophobic
Powders
Perfluoro copolymer
Pyrolysis
Ultra-fine dry chemical agent
Fire re-ignition

ABSTRACT

The re-ignition of pool fires is a common hazard phenomenon in fire extinguishing. Dry chemicals with oleophobicity may solve this problem because powders can float on the oil surface and prevent evaporation of fuel pool. In this research, MAPP (modified ammonium polyphosphate) with superhydrophobicity, oleophobicity, and higher chemical activity is prepared which can quickly quench pool fires and provide longer protection. The activation indexes of MAPP for water, diesel, aviation kerosene and gasoline are 98.5%, 87.4%, 98.7% and 98.4%, respectively. Lower activation energy of MAPP means that it will show higher chemical activity in fire. The fire-extinguishing performance of MAPP is much higher than that of Commercial UDCA (ultra-fine dry chemical agent) during fire experiments. After extinguished by MAPP, the fuel pool is hard to be re-ignited. The significance of this study is to propose a new strategy for preventing the re-ignition of pool fires.

1. Introduction

In case of pool fires, the re-ignition often occurs and can cause big accidents. Sometimes, though the fire has already been extinguished, the pool oil is easily ignited by sparks or other energy as the fuel gas is still evaporating. Halons compounds have been widely used as a gas fire extinguishing agent due to their high efficiency of fire extinguishing. However, the destructive effects on the ozone layer caused them to be banned [1,2]. UDCA is obtained by refining of dry powders and specially treated, usually using ammonium phosphate or carbonate as raw material. UDCA has been thought to be the replacement of Halons since P.Laffitte found that fine powders had better fire suppressing effect than normal size powders [3]. After that, researchers had performed much studies related to the possibility of replacing Halons [4–8]. However,

* Corresponding authors.
E-mail addresses: yyfu@ustc.edu.cn (Y. Fu), lusong@ustc.edu.cn (S. Lu).

https://doi.org/10.1016/j.jhazmat.2019.05.018
Received 21 March 2019; Received in revised form 9 May 2019; Accepted 11 May 2019
Available online 05 July 2019
0304-3894/

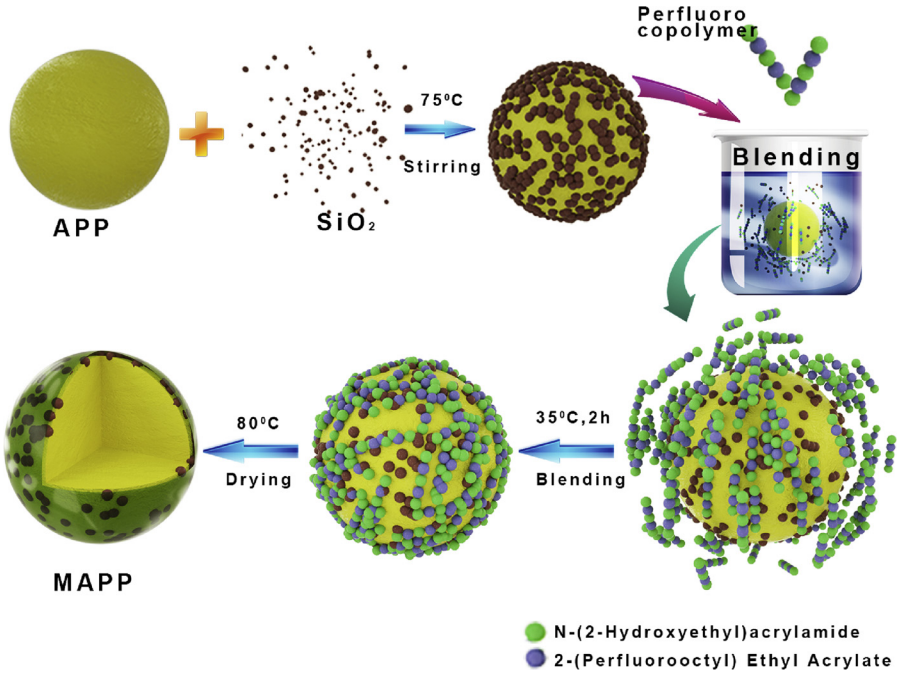

Fig. 1. Schematic illustration of superhydrophobic and oleophobic functional modification of APP particles.

smaller particle size will lead to higher surface energy and the powders will be easier to absorb moisture and deteriorate [9]. Thus, the existing ultra-fine dry chemical agents are mostly subjected to hydrophobic treatment in order to avoid agglomeration during storage.

However, neither Halons nor UDCA can effectively solve the problem of re-ignition of pool fires because of their limited protection time (gas fire extinguishing agents are diluted in the air and dry powder particles will settle). To solve this problem, MAPP with superhydrophobicity, oleophobicity, and higher chemical activity is prepared in this research. Here, ultra-fine APP is used to prepare UDCA for its good ability to extinguish ABC fires. APP has been studied much and mainly focusing on improving the carbonization and material compatibility of APP to improve the heat and smoke release [10–12]. Peikun Zhang fabricated hydroxyl-decorated APP (OH-APP) through a facile, yet efficient cation exchange reaction with N-methylethanolamine, and utilized as a reinforcing agent for PU. Results demonstrate that the conjugation of OH-APP imparts to the resultant cured PU samples (PU/OH-APP) enhanced fire safety and smoke suppression performance [13]. Cong Deng prepared a highly-efficient mono-component polymeric intumescent flame retardant, piperazine-modified ammonium polyphosphate (PA-APP), which was used for polypropylene (PP) [14]. Bihe Yuan studied the effects of graphene on the flammability of intumescent flame retardant polypropylene composites and found that lower loading and well dispersion of graphene will help to improve the swelling of char and decrease in heat and smoke release [15,16]. However, it is hardly to be seen the oleophobic modification of APP as fire suppressants.

William R. Warnock and Donald V. Flatt firstly mentioned in their patent that the use of fluorocarbon surfactants to improve oleophobicity of the dry chemicals' surface, which could provide longer fire protection [17]. But the patent didn't mention the oleophobic performance on oil surface. It is found that the powders prepared by the same method could not fully meet the demand. The powders will fall below the oil surface in large amount under vibration. This means that the powders are not suitable for the protection of pool fires in moving scenarios, such as a moving train and a flying plane. Through literatures review, superhydrophobic and oleophobic materials have been widely studied, such as self-cleaning clothes [18–20], self-cleaning coatings [21–23], anti-fouling films [24–26]. Only little attention had been paid to the hydrophobicity and oleophobicity of powders. Many attempts show three difficulties here: 1. Particles need to have both hydrophobicity and oleophobicity. 2. For a separate particle, the larger the particle, the greater the repulsive force that needs to be provided. Currently Commercial UDCAs are mainly micron-sized carbonates or ammonium phosphates. 3. The activation index in the oil should be high under vibration.

In this paper, we synthesized MAPP powders with superhydrophobicity, oleophobicity, and higher chemical activities. The fire extinguishing experiments shows that MAPP powders have a better fire extinguishing efficiency and provides longer protection than Commercial UDCA.

2. Experimental section

2.1. Materials

All reagents were used as received from chemical reagent companies without any further purification. Tetrahydrofuran, 1, 1, 2-trichloroethane were purchased from China National Pharmaceutical Group Corporation. SiO_2, azobisisobutyronitrile, and N-(2-hydroxyethyl) acrylamide were purchased from Aladdin Co., Ltd. 2-(perfluorooctyl) ethyl acrylate was purchased from Quzequan Co., Ltd. The ultra-fine MAPP was bought from Shandong Jingxin Powders Co., Ltd. The dispersed machine was a 5 L reactor supplied by Henan Yingyu Co., Ltd. The aviation kerosene type was RP-3, and both gasoline and diesel were purchased from China Petrochemical Corporation.

2.2. Preparation of MAPP

Fig. 1 shows the preparation process of MAPP. The perfluoro copolymer is synthesized by radical polymerization using 30% of perfluorooctylethyl acrylate and 70% of N-(2-hydroxyethyl) acrylamide as raw materials. The whole process lasts for 10 h under the protection of nitrogen at the temperature of 50–75 °C. APP (95%, wt) and silica (5%, wt) are dispersed at 75 °C for 2 h. The obtained powders (95%, wt) are mixed with the perfluoro copolymer (5%, wt) in tetrahydrofuran and hydrogen bonds(it will be proved below) are formed with the amide group and APP at 35 °C [27]. During the process of drying at 80 °C, the

perfluoro copolymer melts on the surface of APP and further crosslinks. The perfluoro copolymer changes from a long chain structure into a spatial network structure. Then, APP surface is successfully encapsulated. The obtained MAPP can be both hydrophobic and oleophobic, and have high activation indexes in water and oil.

2.3. Characterizations

The particle size distribution was measured using SALD-2300 of Shimadzu Corporation of Japan. The Fourier infrared spectroscopy test machine was produced by METTLER. The SU8220 cold field emission scanning electron microscope was used to observe the microstructure of the MAPP particles. The TGA-DSC machine was manufactured by PerkinElmer.

2.4. Experimental details

The fire suppression test was carried out in a standard fire test room (4 m × 4 m × 3.7 m). The volume of the dusting device is 900 ml. The fuel pan is 40 cm × 40 cm. The diameter of the powder spraying nozzle is 2 mm. The Sony 4 K camera is used for imaging. The ignitor was purchased from Shanxi Qinchuan Thermal Technology Co., Ltd.

3. Results and discussion

3.1. Structural analysis, hydrophobicity and oleophobicity

UDCA has a better fire-extinguishing performance than Halons, which has been tested by G.C. Harrison [4]. The D_{90} (90% of the cumulative distribution of particle size) particle size of UDCA should be less than 20 μm, which has been mentioned by Curtis T. Ewing [5]. Here, APP is used as a raw material for fire extinguishing agents due to its good thermal stability and wide application range [10]. Fig. 2a shows the particle size distribution of APP and MAPP. The D_{90} of APP and MAPP are 1.007 μm and 1.028 μm, respectively. It can be seen that D_{90} of APP and MAPP are much smaller than 20 μm and the particle size distribution changes little after modification. Fig. 2b shows the FTIR spectra of the perfluoro copolymer. The disappearance of the peak of the double bond of carbon near 1600 cm^{-1} proves that polymerization occurs. At 660 cm^{-1} and 1560 cm^{-1}, the deformation vibration of N—H is observed, and the stretching vibration of N—H is observed at 3350 cm^{-1}. The presence of carbonyl group (—C = O—) in the amide group is observed in 1650 cm^{-1}. It confirms the presence of the amide group (—CO—NH—). At 1735 cm^{-1}, it is the stretching of carbon-oxygen double bond (C═O). It can be observed that the two stretching vibration absorption peaks of the ether bonds are at 1138 cm^{-1} and 1204 cm^{-1}. At 3400 cm^{-1}, the stretching vibration of hydroxyl (—OH) can be observed. The out-of-plane bending vibration of C–H is observed at 710 cm^{-1} and the asymmetric stretching peak of CH_2 is observed between 2850 cm^{-1} and 2940 cm^{-1}. Symmetrical stretching peaks of carbon-hydrogen bond (C–H) can be observed at 1380 cm^{-1} and 1460 cm^{-1}. At 1060 cm^{-1}, it is the out-of-plane bending of C–H. The C–F bond is observed at 1344 cm^{-1}. It can be seen from Fig. 2c that the peak of APP is mainly concentrated at 3000 cm^{-1} 3400 cm^{-1} (N—H symmetric stretching vibration), 1250 cm^{-1} (symmetrical stretching vibration of P═O), 1070 cm^{-1} (symmetric stretching vibration of P—O), 884 cm^{-1} (asymmetric stretching vibration of P—O) and 1016 cm^{-1} (symmetric stretching vibration of PO_2 and PO_3). Compared to APP, in addition to the peaks described above, MAPP forms N—H deformation vibration at 1557 cm^{-1}. At 1600 cm^{-1}–1782 cm^{-1} and 3000 cm^{-1}–3400 cm^{-1}, the peak strength is increased due to the encapsulation of polymer. However, since the peak of C–F is covered by other peaks (P═O, N—H), so it is not observed. The surface elements of the perfluoro copolymer, APP, MAPP, respectively are shown in Fig. 2d. The F 1s peak appears in MAPP but it can't be seen on the surface of APP. The high resolution spectrum of N 1s spectrum of MAPP shows two peaks at 399.4 eV and 401.1 eV, respectively. The high binding energy signal (401.1 eV) observed in the XPS can be attributed to hydrogen bond or protonated nitrogen and the low binding energy signal (399.4 eV) to free amines [28]. The result demonstrates that MAPP was encapsulated by the perfluoro copolymer through hydrogen bond. Fig. 2e1 shows that the perfluoro copolymer forms particle aggregation state at a microscopic level. Upon amplification, cross-linking of the particles can be seen in Fig. 2e2. And Fig. 2e3, APP powders form a smooth surface, which is different with MAPP. Fig. 2e4 shows the surface of MAPP is coated with a layer of gel after modification by the perfluoro copolymer. F element is the most electronegative element in nature, and the C–F bond has strong hydrophobicity and oleophobicity [29–31]. Due to the presence of the fluorine-containing gel layer, when placed in water/oil, the gel layer coated on the surface of the particles repels with liquids, making it difficult to be wetted.

Fig. 3a reveals the hydrophobic and oleophobic mechanisms of the MAPP powders. The long PFD chains (long chain containing $–(CF_2)_7CF_3$ moiety) lead to a change in the nature of surface asperities along with lowering of effective surface energy (due to very low surface energy of PFD moiety) [32]. When the powders contact with water/ oil surface, the repulsive force between the PFD chains and the water/oil will keep powders from being wetted. Due to the non-uniformity of fluorine-containing gel layers on the surface of a separate particle, the roughness is increased, which also contributes to the improvement of the hydrophobicity and oleophobicity of MAPP powders. However, the low surface tension liquid may also wet powders through this defect. When the water/oil droplets are dropped onto the MAPP surface, the low surface energy of the powders and the surface arrangement have both effects on the hydrophobicity and oleophobicity. Thus, two indicators of CA (contact angle) and activation index are used to characterize the hydrophobicity and oleophobicity of MAPP.

Fig. 3b shows the wetting properties of four droplets: water, gasoline, diesel, and aviation kerosene on the surface of MAPP. Four types of the droplets appeared spherical on the surface of MAPP. Here, deionized water is used to examine the hydrophobicity and gasoline, diesel, and aviation kerosene are used to examine the oleophobicity of MAPP. Gasoline and diesel are common fuels for automobiles and aviation kerosene is often used in ships and airplanes [33–35]. Comparison of the three fuels will make the results more meaningful. Fig. 3c shows the contact angle measurement. It can be seen that the hydrophobic angle is 155.2°, which can be considered as superhydrophobic (CA > 150°) [36–38]. Fig. 3c2, 3c3 and 3c4 are contact angle measurements of diesel, gasoline and aviation kerosene, respectively. Among the three kinds of oil, the surface tension of gasoline is lowest [39], and CA of gasoline is 131.5°,which is the lowest. The contact angles of diesel and aviation kerosene are 137.6° and 136.5°, respectively. In the actual fire extinguishing experiment, the activation index of powders on the oil surface is very important which is introduced by Xiaojing Zhang's experiments [40]. Here, the same method is used to characterize the hydrophobicity and oleophobicity of MAPP. The activation index is calculated by Eq. (1):

$$\text{Activation index}\,(\%) = \frac{W}{5} * 100\,\% \tag{1}$$

Here, W is the weight of the powders recovered from floating on the liquids. The final activation index of the particles is an average value.

MAPP of 5.000 + 0.02 g is weighed into a beaker containing 30 ml of liquids, and the residual amount of MAPP before and after stirring are shown in Fig. 3d5, 3d6, 3d7, 3d8. Fig. 3e shows the activation indexes of MAPP powders obtained after the floating powders are weighed. For water, diesel and aviation kerosene, the activation indexes are all over 98%. Due to the low surface tension of the gasoline (21.56 $mN{\cdot}m^{-1}$) [39], the activation index of MAPP for gasoline is only 87.4%.

The other physical properties tests of MAPP are given in Table 1. The indicators are measured in accordance with the test standards of ISO 7202-2018 [41]. In conclusion, the obtained MAPP has excellent

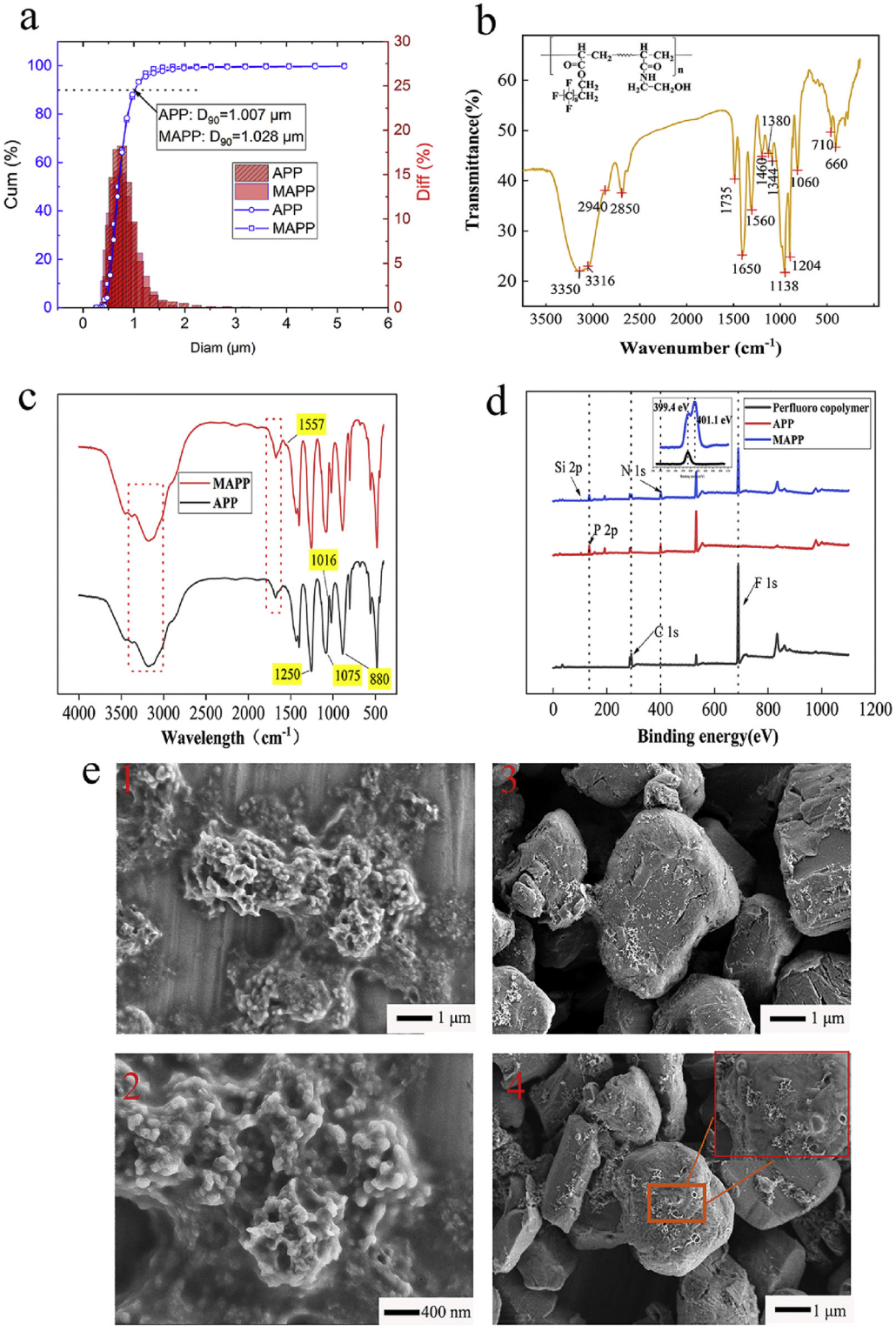

Fig. 2. a) The particle diameter distribution of APP and MAPP. b) FTIR spectra of the perfluoro copolymer. c) Comparison of FITR spectra of APP and MAPP. d) XPS characterizations of the perfluoro copolymer, APP and MAPP. e) SEM images: (1) The perfluoro copolymer dispersed with ethanol. (2) The enlarged graph of the perfluoro copolymer. (3) APP dispersed with ethanol. (4) MAPP dispersed with ethanol.

properties, and the test values are higher than the prescribed standards.

3.2. Pyrolysis process

Thermal analysis kinetics is an important approach to study the mechanisms of thermochemical conversion of the materials. Non-isothermal kinetics was used to determine the activation energy and the conversion mechanism of the perfluoro copolymer. The model-free method, also called the iso-conversional method, was the most common used methods in the kinetics study of polymer pyrolysis process [42–44]. The ICTAC Kinetic Committee recommended that using multiple heating rate programs would obtain more reliable kinetic

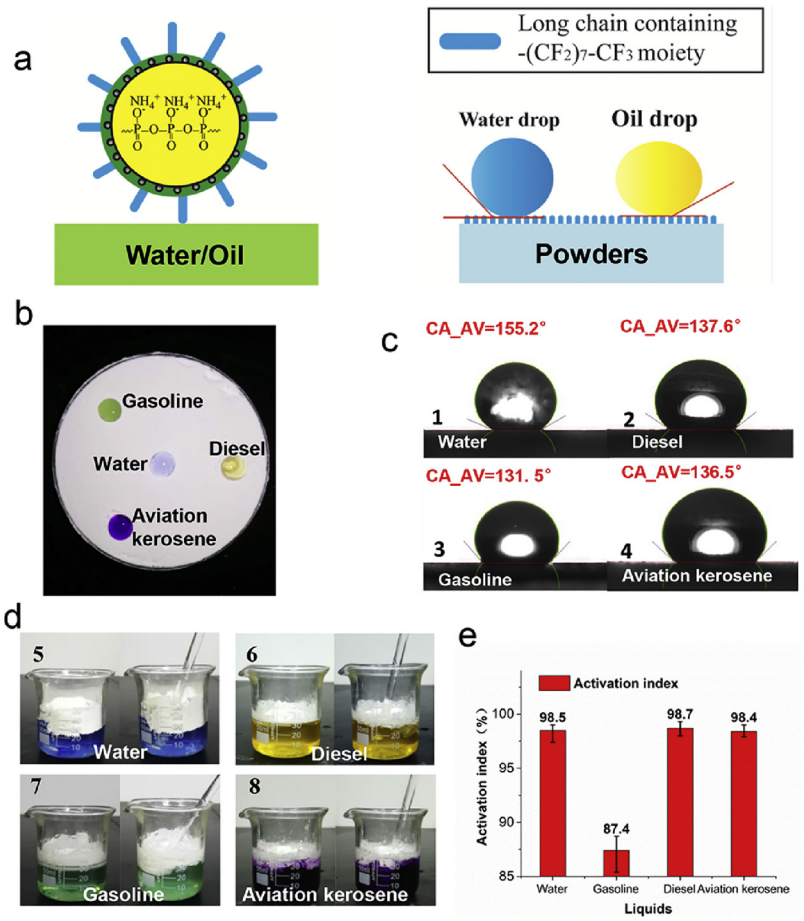

Fig. 3. Schematic illustration of hydrophobic and oleophobic properties of MAPP: a) Hydrophobic and oleophobic mechanisms of MAPP. b) Wetting characteristics of four liquids (water, diesel, gasoline, aviation kerosene) on the surface of MAPP powders. c) CA of MAPP powders for four liquids (water, diesel, gasoline, aviation kerosene). d) Activation index measurements of MAPP powders (stirring for 10 min). e) Activation indexs of MAPP powders in four liquids.

parameters instead of single heating rate program [45]. For this method, the essential assumption is that the reaction rate for a constant extent of conversion (α) depends only on the temperature (T). Here, Kissinger–Akahira–Sunose equation is used to analyze the pyrolysis process, which is shown in Eq. (2):

$$\ln\frac{\beta}{T^2} = \ln\frac{AEa}{RG(\alpha)} - \frac{Ea}{RT} \quad (2)$$

Here, β, T and A represents the heating rate, temperature and pre-exponential factor. Ea is the activation energy, R = 8.314 J·mol^{-1} K^{-1}, the ideal gas constant; G(α) is a function of α. When α is constant, G(α) is constant [45–47].

For APP and MAPP, the pyrolysis processes are analyzed. The TG curves in Fig. 4a and b show that both APP and MAPP undergo a two-step thermal degradation process in nitrogen atmosphere. Since APP mainly undergoes pyrolysis reactions during the heating process, only nitrogen atmosphere is used here. As shown in Fig. 5, the evolved products at Step 1 are mainly ammonia and water, while the polyphosphoric acid is generated. For MAPP, the initial decomposition temperature is 288.72 °C, which is a bit higher than that of APP (280.02 °C). This illustrates that MAPP decomposes later than APP. Step 2 is the main decomposition processes of APP and MAPP. For APP, a rapid mass loss rate at 655.35 °C is detected, which is regarded as the breakdown of the ultraphosphate structure and the formation of volatile P_2O_5 [48]. For MAPP, the temperature at maximum weight loss rate of MAPP (606.38 °C) is lower than that of APP (655.35 °C). This can be explained by the reactions of hydroxyethyl between perfluoro copolymers and APP, which promotes the elimination of water in Step 2 [49]. So, the gas products are allowed to leave the solid phase at a lower temperature [48]. The effect of the perfluoro copolymer on the pyrolysis phase of APP can also be reflected in the calculation of Ea. Here, heating rates of 10 °C/min, 20 °C/min, 30 °C /min and 40 °C/min are used. Figs. 4c and d show good fittings of data, which demonstrate the reliability.

As can be seen from Fig. 6, Ea of Step 1 of MAPP is higher than that of APP. However, since the mass loss of Step 1 is 18.5%, which is much smaller than 49.7% of Step 2, it can be considered that Step 2 is dominant in the thermal mechanism of the fire extinguishing. The lower Ea of Step 2 means that MAPP will be easier to decompose and perform better fire extinguishing effects than APP. Step 3 shows that Ea of both of APP and MAPP tends to be stable and the decomposition stop.

3.3. Fire-fighting efficiency and mechanisms

The fire extinguishing experiments is carried out for gasoline, aviation kerosene and diesel pool fires. Details of the experimental apparatus are schematically shown in Fig. 7d. The 400 ml oil liquid is contained in the oil pan with the diameter of 0.40 m. In each test,

Table 1
Test values of physical properties of MAPP *vs.* standard values.

Categories	Water repellency	Penetration [mm]	Bulk density [g/ml]	Moisture content [%]	Moisture absorption rate [%]
MAPP	Excellent	29.27	2.14	0.15	1.42
Standard values		≥25.00	≥0.82	≤0.25	≤2.00

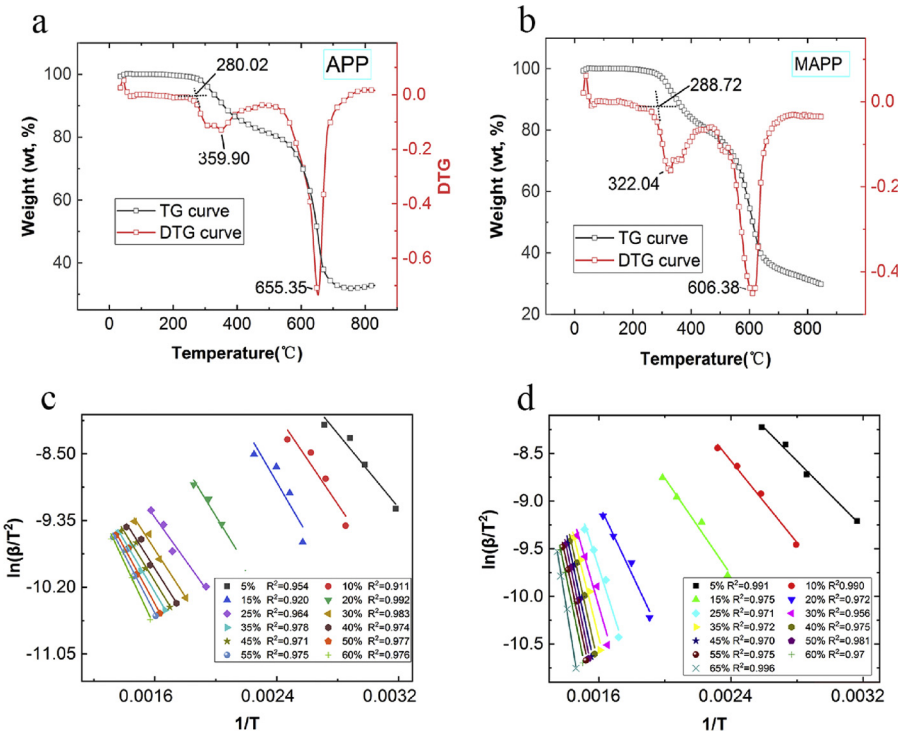

Fig. 4. a) TG and DTG curves of APP in nitrogen atmosphere (Heating rate: 10 °C/min). b) TG and DTG curves of MAPP in nitrogen atmosphere (Heating rate: 10 °C/min). c) Curves of $\ln[\beta/T^2]$ *vs.* 1/T for APP in nitrogen atmosphere at multiple conversion rates. d) Curves of $\ln[\beta/T^2]$ *vs.* 1/T for MAPP in nitrogen atmosphere at multiple conversion rates.

Step 1: $(NH_4)_nP_nO_{3n+1} \triangleq H_3PO_4 + NH_3\uparrow$

Step 2: $3\,H_3PO4 \triangleq H_3P_3O_9 + 3H_2O\uparrow \rightarrow (HPO_3)_n$

Fig. 5. The two steps of pyrolysis process of APP and MAPP.

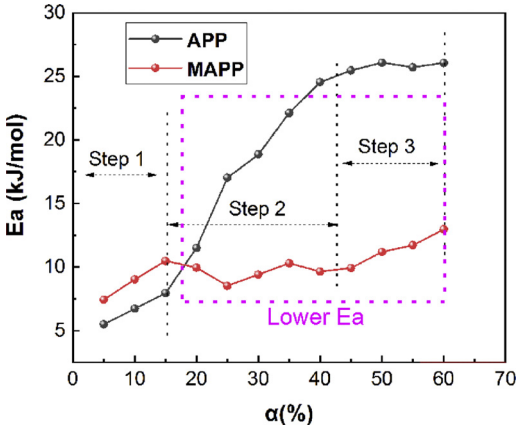

Fig. 6. Evolution of Ea of APP and MAPP during pyrolysis process under nitrogen atmosphere.

200.0 g powders were added into a tank with the volume of 900 ml and pressurized by nitrogen to a pre-assigned value of 1.20 MPa. Before powder discharging, 400 ml gasoline was added into the pan, ignited and pre-burned for 30 s. The distance and angle from the extinguisher nozzle to the pan center was set as 1.0 m and 30°, respectively. The valve of the powder tank was turned off as soon as the fire was extinguished. The weight of the tank was measured before and after each test to determine the total mass of suppressants consumed for fire extinguishment. Each test was repeated at least three times to get a converged result. The fire suppression process was recorded by a video camera.

As can be seen from Fig. 7a, small difference is found in extinguishing diesel and kerosene pool fires. When the gasoline and aviation kerosene fires have been extinguished by MAPP, the flame can still be seen in the process of the Commercial UDCA extinguishing. The main difference is reflected in the extinguishing process of the gasoline pool fires. The low flash point and evaporation temperature make gasoline burn more severely. Fig. 7a shows that the Commercial UDCA needs more than 4 s for extinguishing gasoline pool fire, while MAPP only needs 1.6 s. Table 2 lists the agent mass consumed in fire tests. It can confirm that MAPP exhibits much better fire extinguishing performance than Commercial UDCA. Particularly, the agent mass consumed in extinguishing gasoline pool is 71.5 g, while Commercial UDCA mass consumed is 139.7 g, which corresponds to the fire extinguishing time. Fig. 7b shows the comparison of the oil surface after fire extinguishing by Commercial UDCA and MAPP. After extinguishing by Commercial UDCA, there is no powders residue on the oil surface. After fire extinguishing completed by MAPP, the surfaces of oil are covered by MAPP powders. In order to test its re-ignition effect, re-ignition tests are performed using 17 J of ignition energy. It can be observed from Fig. 7c that the gasoline pool fire that has been extinguished by Commercial UDCA will be re-ignited within 1 s. For the gasoline pool fire extinguished by MAPP, the ignition process needs more than 20 s, and it still cannot re-ignite the pool oil. The covering MAPP of the oil surface can effectively prevent the evaporation of oil gas, thereby providing long-term protection after the flame is extinguished.

Detailed analysis of the fire extinguishing mechanism of MAPP is given in this article. The first is the effect of asphyxiation. The oleophobicity of MAPP plays a very important role during the fire extinguishing process. When the oleophobic powders enter the flame zone and contact the oil, they can cover the oil surface of the oil, thereby forming an insulation layer, inhibiting evaporation of the fuel and preventing the combustion reaction. Affected by the heating of the flame zone, MAPP decomposes NH_3 and H_2O, which will absorb heat from the flame zone and lower the temperature in the flame zone. NH_3 and H_2O exist in gasous phase due to the high temperature in the flame zone. Thus, they can dilute the concentration of oxygen and reduce the severity of flame combustion.

Spread of flame inside a combustible gaseous mixture is caused by the so-called 'chain' exothermic reactions, *i.e.* competing reactions

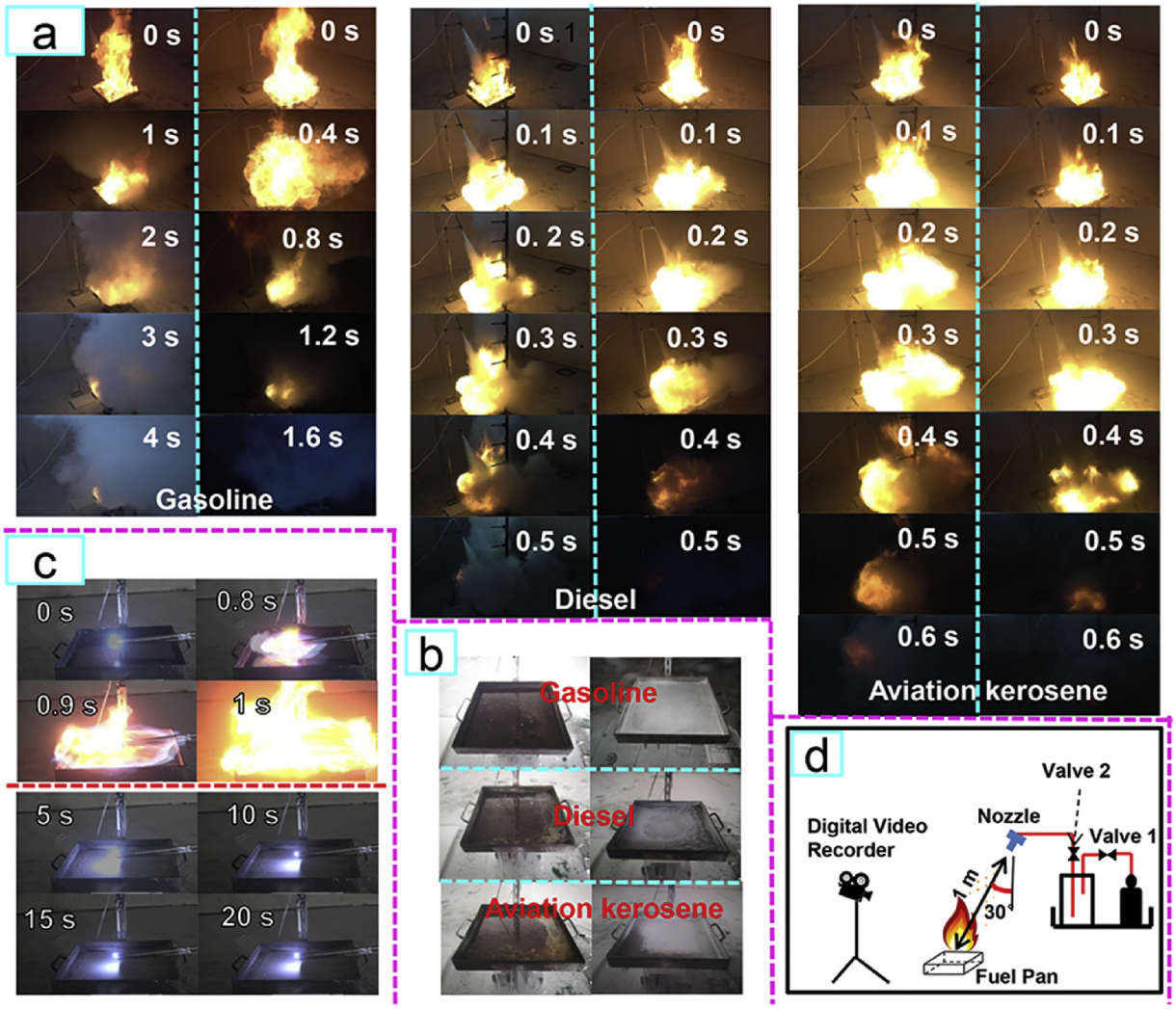

Fig. 7. Fire-fighting and re-ignition experiments: a) Comparison of Commercial UDCA and MAPP fire extinguishing process for three different pool oil fires (The left column is the Commercial UDCA, and the right column is MAPP). b) Comparison of surface condition of Commercial UDCA and MAPP after fire extinguishing. c) Comparison of gasoline pool re-ignition experiments after fire-fighting (The up four pictures are suppressed by Commercial UDCA, and the four pictures below are suppressed by MAPP; the electric sparking energy is 17 J). d) Fire-fighting experiments set-up.

Table 2
Mass of Commercial UDCA and MAPP consumed in extinguishing pool fires.

Agents	Fuel	Mass loss of agents [g]			Average mass loss [g]
		Test 1	Test 2	Test 3	
Commercial UDCA	Gasoline	157	132	130	139.7
	Diesel	28.1	27.4	25.1	26.9
	Aviation kerosene	28.6	29.1	28.8	28.8
MAPP	Gasoline	79.5	54	81	71.5
	Diesel	25.6	18.5	20.1	21.4
	Aviation kerosene	23.8	13.2	10.7	15.9

between active atoms (or 'molecular fragments') of the flame (the so-called 'flame free radicals' (FFR)) [33,50]. The chemical mechanism of UDCA in fire extinguishing can be divided into two categories: one is FFR attacking in the gas phase, and the other is chemical adsorption in the [solid surface-gas] systems [50]. For gas phase, NH_3/NH_2 and HF/F· can attack FFR and prevent the chain reaction from proceeding. As seen from Fig. 8, the front end of the flame is relatively high in H_2/·OH, and thus the reaction of H· with the competitor is the most important fire inhibiting reaction [51]. For [solid surface-gas] systems, chemi-adsorbed FFR by the active centers of cluster surface (ACCS) and FFR reaction with $[PO_4]$ group. A detailed explanation is given here in Fig. 8. Defects on the surface of MAPP particle can form chemical active centers. The ACCS can chemically adsorb a large amount of FFR and attack the FFR in the flame. Due to the movement of the MAPP particles and the decomposition process, oscillating relaxation process (accommodation of energy during recombination) will be happened in MAPP particle. The decomposition of MAPP will cause the $[PO_4]$ group to be exposed to the surface of the powder to attacking FFR, thereby improving the fire extinguishing effect. Compared with Commercial UDCA, the reason of higher MAPP's fire extinguishing efficiency is mainly reflected in the asphyxiation of flame and the reaction of HF/F· system with FFR.

4. Conclusions

In this study, a perfluoro copolymer is synthesized which used perfluorooctylethyl acrylate and N-(2-hydroxyethyl) acrylamide as raw materials. Structure, hydrophobicity and oleophobicity of powders have been analyzed. The important results of this article are listed as follows:

(1) Develop a simple way to impart APP powders to be both superhydrophobic and oleophobic. The new fire suppressants (MAPP)

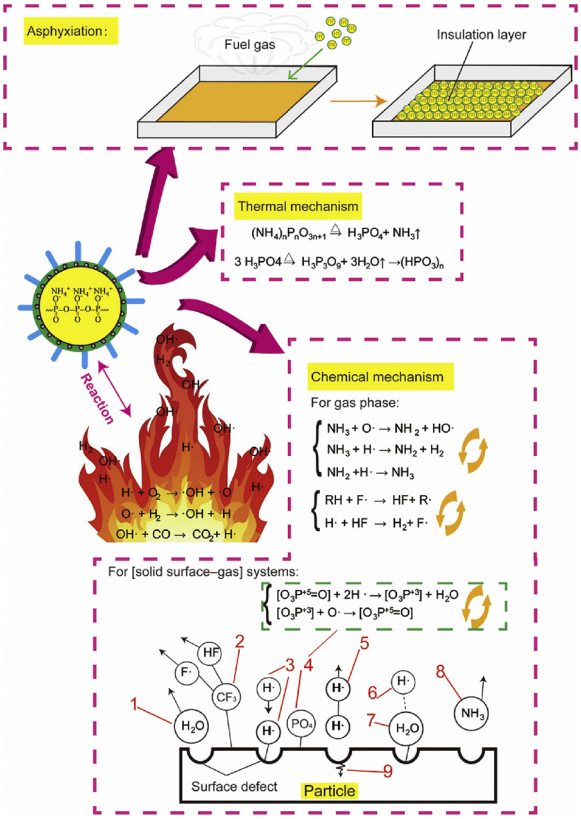

Fig. 8. The fire-fighting mechanism of MAPP: (1) The desorption of water. (2) Decomposition process of fluorinated branches on the surface of MAPP. (3) Chemi-adsorbed and attacking FFR. (4) $[PO_4]$ groups exposed on the surface of MAPP. (5) H_2 desorption molecule (product of recombination reaction). (6) FFR, chemi-adsorbed by adsorption layer. (7) Adsorption layer. (8) The desorption of NH_3. (9) Oscillating relaxation process in MAPP particle (accommodation of energy during recombination).

provided a new strategy for preventing the re-ignition of pool fires. The activation indexes of MAPP for water, diesel, aviation kerosene and gasoline are 98.5%, 87.4%, 98.7% and 98.4%, respectively. Excellent hydrophobic and oleophobic properties will ensure the effectiveness of fire extinguishing in a variety of situations.

(2) The obtained MAPP has a lower Ea and can perform a higher chemical activity in fire. The obtained MAPP has excellent properties, and the test values are much higher than the standard values of ISO 7202-2018.

(3) Compared to Commercial UDCA, the thermal and chemical mechanisms during fire extinguishing are improved. The oleophobicity allows the powders to form an oleophobic layer on the fuel surface, and the fuel evaporating is greatly reduced, which also promotes the improvement of the MAPP fire-extinguishing performance. The presence of the oleophobic layer also reduces the chance of re-ignition of the fuel.

In general, the designed and synthesized MAPP is simple to prepare, has superhydrophobicity, oleophobicity, higher chemical activity and can provide a longer time protection. The MAPP can be used in varieties of applications to improve fire protection, such as small gas stations, airports, aircraft engine nacelle, *etc.*

Acknowledgements

This work was supported by the National Key R&D Program of China (No. 2018YFC0807605-1) and the National Natural Science Foundation of China (No. 51804288).

Appendix A. Supplementary data

Supplementary material related to this article can be found, in the online version, at doi:https://doi.org/10.1016/j.jhazmat.2019.05.018.

References

Hynes, R.G., Mackie, J.C., Masri, A.R., 1999. Shock-tube study of the pyrolysis of the halon replacement molecule CF3CHFCF3. J. Phys. Chem. A 103, 54–61 %@ 1089-5639.
Molina, M.J., Rowland, F.S., 1974. CFCs in the environment. Nature 8.
Laffitte, P., Delbourgo, R., Combourieu, J., Dumont, J.C., 1965. The influence of particle diameter on the specificity of fine powders in the extinction of flames. Combust. Flame 9, 357–367 %@ 0010-2180.
Harrison, G.C., 1993. Solid Particle Fire Extineuishants for Aircraft Auulications.
Ewing, C.T., Faith, F.R., Romans, J.B., Hughes, J.T., Carhart, H.W., 1992. Flame extinguishment properties of dry chemicals: extinction weights for small diffusion pan fires and additional evidence for flame extinguishment by thermal mechanisms. J. Fire Prot. Eng. 4, 35–51 %@ 1042-3915.
Ewing, C.T., Faith, F.R., Hughes, J.T., Carhart, H.W., 1989. Flame extinguishment properties of dry chemicals: extinction concentrations for small diffusion pan fires. Fire Technol. 25, 134–149 %@ 0015-2684.
Jiang, Z., Chow, W.K., Li, S.F., 2007. Review on additives for new clean fire suppressants. Environ. Eng. Sci. 24, 663–674.
Yan, Y., Han, Z., Zhao, L., Du, Z., Cong, X., 2018. Study on the relationship between the particle size distribution and the effectiveness of the K-powder fire extinguishing agent. Fire Mater. 42, 336–344.
Yingxin, L.J.R., 2003. Application of surfactants in preparation of nano-particle. New Chem. Mater. 7, 011.
Castrovinci, A., Camino, G., Drevelle, C., Duquesne, S., Magniez, C., Vouters, M., 2005. Ammonium polyphosphate–aluminum trihydroxide antagonism in fire retarded butadiene–styrene block copolymer. Eur. Polym. J. 41, 2023–2033 %@ 0014-3057.
Chen, S., Li, X., Li, Y., Sun, J., 2015. Intumescent flame-retardant and self-healing superhydrophobic coatings on cotton fabric. ACS Nano 9, 4070–4076 %@ 1936-0851.
Realinho, V., Haurie, L., Formosa, J., Velasco, J.I., 2018. Flame retardancy effect of combined ammonium polyphosphate and aluminium diethyl phosphinate in acrylonitrile-butadiene-styrene. Polym. Degrad. Stab. 155, 208–219 %@ 0141-3910.
Zhang, P., Zhou, Y., Su, H., Lin, H., Tian, S., Chen, Y., Yan, J., He, Y., Fan, H., 2017. Hydroxyl-decorated ammonium polyphosphate as flame retardant reinforcing agent in solvent-free two-component polyurethane. Polym. Int. 66, 1598–1609 %@ 0959-8103.
Wang, Q., Undrell, J.P., Gao, Y., Cai, G., Buffet, J.-C., Wilkie, C.A., O'Hare, D., 2013. Synthesis of flame-retardant polypropylene/LDH-borate nanocomposites. Macromolecules 46, 6145–6150 %@ 0024-9297.
Yuan, B., Fan, A., Yang, M., Chen, X., Hu, Y., Bao, C., Jiang, S., Niu, Y., Zhang, Y., He, S., 2017. The effects of graphene on the flammability and fire behavior of intumescent flame retardant polypropylene composites at different flame scenarios. Polym. Degrad. Stab. 143, 42–56 %@ 0141-3910.
Yuan, B., Sun, Y., Chen, X., Shi, Y., Dai, H., He, S., 2018. Poorly-/well-dispersed graphene: abnormal influence on flammability and fire behavior of intumescent flame retardant. Compos. Part A Appl. Sci. Manuf. 109, 345–354 %@ 1359-1835X.
W.R. Warnock, D.V. Flatt, J.R. Eastman, Anti-reflash dry chemical agent, in, Google Patents, 1971.
Moiz, A., Padhye, R., Wang, X., 2017. Coating of TPU-PDMS-TMS on polycotton abrics for versatile protection. Polymers 9, 1–17 %@ 2073-4360.
Grethe, T., Kick, T., Mahltig, B., 2017. Sustainable controlling of hydrophilic properties of cotton and linen by application of amino acids. J. Text. Inst. 108, 436–439 %@ 0040-5000.
Abidi, N., 2018. chemical properties of Cotton fiber and chemical modification. Cotton Fiber: Physics, Chemistry and Biology. Springer, pp. 95–115.
Bouvet-Marchand, A., Graillot, A., Abel, M., Koudia, M., Boutevin, G., Loubat, C., Grosso, D., 2018. Distribution of fluoroalkylsilanes in hydrophobic hybrid sol-gel coatings obtained by co-condensation. J. Mater. Chem. A.
A. Kessman, D. Cairns, Hydrophobic and oleophobic coatings, in, Google Patents, 2018.
Rocha Canella Carneiro, A., de Souza Ferreira, F.A., Houmard, M., 2018. Easy functionalization process applied to develop super-hydrophobic and oleophobic properties on ASTM 1200 aluminum surface. Surf. Interface Anal %@ 0142-2421.
Kwak, S.-Y., Kim, S.H., Kim, S.S., 2001. Hybrid organic/inorganic reverse osmosis (RO) membrane for bactericidal anti-fouling. 1. Preparation and characterization of TiO2 nanoparticle self-assembled aromatic polyamide thin-film-composite (TFC) membrane. Environ. Sci. Technol. 35, 2388–2394 %@ 0013-2936X.
Zhang, X., Tian, J., Gao, S., Zhang, Z., Cui, F., Tang, C.Y., 2017. In situ surface modification of thin film composite forward osmosis membranes with sulfonated poly (arylene ether sulfone) for anti-fouling in emulsified oil/water separation. J. Memb. Sci. 527, 26–34 %@ 0376-7388.
Walker, J.A.-T., Robinson, K.J., Munro, C., Gengenbach, T., Muller, D.A., Young, P.R., Lua, L.H.L., Corrie, S.R., 2018. Antibody-binding, anti-fouling surface coatings based on recombinant expression of zwitterionic EK peptides. Langmuir %@ 0743-7463.
Hagler, A.T., Lifson, S., Dauber, P., 1979. Consistent force field studies of intermolecular forces in hydrogen-bonded crystals. 2. A benchmark for the objective comparison of alternative force fields. J. Am. Chem. Soc. 101, 5122–5130 %@ 0002-7863.
Graf, N., Yegen, E., Gross, T., Lippitz, A., Weigel, W., Krakert, S., Terfort, A., Unger, W.E.S., 2009. XPS and NEXAFS studies of aliphatic and aromatic amine species on functionalized surfaces. Surf. Sci. 603, 2849–2860 %@ 0039-6028.

Lakshmi, R.V., Bharathidasan, T., Bera, P., Basu, B.J., 2012. Fabrication of superhydrophobic and oleophobic sol–gel nanocomposite coating. Surf. Coat. Technol. 206, 3888–3894.
Fabbri, P., Messori, M., Pilati, F., Taurino, R., Tonelli, C., Toselli, M., 2007. Hydrophobic and oleophobic coatings based on perfluoropolyether/silica hybrids by the sol-gel method. Adv. Polym. Technol. 26, 182–190 %@ 0730-6679.
Darmanin, T., Guittard, F., 2015. Superhydrophobic and superoleophobic properties in nature. Mater. Today 18, 273–285 %@ 1369-7021.
Sengupta, A., Malik, S.N., Bahadur, D., 2016. Developing superhydrophobic and oleophobic nanostructure by a facile chemical transformation of zirconium hydroxide surface. Appl. Surf. Sci. 363, 346–355.
Ni, X., Zhang, S., Zheng, Z., Wang, X., 2018. Application of water@silica core-shell particles for suppressing gasoline pool fires. J. Hazard. Mater. 341, 20–27.
Wells, S.P., Cozart, K.S., Mitchell, M.B., Dodsworth, R.D., 1997. Aircraft hangar fire threat study and analysis. Air Force Research Lab Tyndall AFB FL Materials and Manufacturing Directorate.
Li, C., Yao, Y., Tao, Z., Yang, R., Zhang, H., 2017. Influence of depressurized environment on the fire behaviour in a dynamic pressure cabin. Appl. Therm. Eng. 125, 972–977.
Xue, Z., Liu, M., Jiang, L., 2012. Recent developments in polymeric superoleophobic surfaces. J. Polym. Sci. Part B: Polym. Phys. 50, 1209–1224.
Cao, L., Price, T.P., Weiss, M., Gao, D., 2008. Super water-and oil-repellent surfaces on intrinsically hydrophilic and oleophilic porous silicon films. Langmuir 24, 1640–1643 %@ 0743-7463.
Yang, J., Yin, L., Tang, H., Song, H., Gao, X., Liang, K., Li, C., 2015. Polyelectrolyte-fluorosurfactant complex-based meshes with superhydrophilicity and superoleophobicity for oil/water separation. Chem. Eng. J. 268, 245–250.
Wang, F., Wu, J., Liu, Z., 2006. Surface tensions of mixtures of diesel oil or gasoline and dimethoxymethane, dimethyl carbonate, or ethanol. Energy Fuels 20, 2471–2474 %@ 0887-0624.
Zhang, X., Shen, Z., Cai, C., Yu, X., Du, J., Xing, Y., Ma, S., 2012. Modification of ADP extinguishing powder by siliconization in spray drying. Particuology 10, 480–486.
ISO 7202-2018: Fire protection – Fire extinguishing media – Powder, in, ISO, 2018, pp. 34.
Aboulkas, A., El Harfi, K., El Bouadili, A., 2008. Non-isothermal kinetic studies on co-processing of olive residue and polypropylene. Energy Convers. Manage. 49, 3666–3671 %@ 0196-8904.
Agrawal, A., Chakraborty, S., 2013. A kinetic study of pyrolysis and combustion of microalgae Chlorella vulgaris using thermo-gravimetric analysis. Bioresour. Technol. 128, 72–80 %@ 0960-8524.
Ma, Z., Chen, D., Gu, J., Bao, B., Zhang, Q., 2015. Determination of pyrolysis characteristics and kinetics of palm kernel shell using TGA–FTIR and model-free integral methods. Energy Convers. Manage. 89, 251–259 %@ 0196-8904.
Vyazovkin, S., Burnham, A.K., Criado, J.M., Pérez-Maqueda, L.A., Popescu, C., Sbirrazzuoli, N., 2011. ICTAC Kinetics Committee recommendations for performing kinetic computations on thermal analysis data. Thermochim. Acta 520, 1–19 %@ 0040-6031.
Jeziorny, A., 1978. Parameters characterizing the kinetics of the non-isothermal crystallization of poly (ethylene terephthalate) determined by DSC. Polymer 19, 1142–1144 %@ 0032-3861.
Budrugeac, P., 2002. Differential non-linear isoconversional procedure for evaluating the activation energy of non-isothermal reactions. J. Therm. Anal. Calorim. 68, 131–139 %@ 1388-6150.
Camino, G., Grassie, N., McNeill, I.C., 1978. Influence of the fire retardant, ammonium polyphosphate, on the thermal degradation of poly (methyl methacrylate). J. Polym. Sci.: Polym. Chem. Ed. 16, 95–106 %@ 0360-6376.
Hu, S., Sun, W.W., Chen, F., 2015. Effect of Aluminium hydroxide and α–SiO2 on thermal decomposition of ammonium polyphosphate. J. Chin. Ceram. Soc. 43, 809–816.
Krasnyansky, M., 2008. Studies of fundamental physical–chemical mechanisms and processes of flame extinguishing by powder aerosols. Fire Mater 32, 27–47 %@ 0308-0501.
Morgan, A.B., Wilkie, C.A., 2007. Flame Retardant Polymer Nanocomposites. John Wiley & Sons.